GAS MOLECULAR EN CUATRO GALAXIAS ESPIRALES BARREADAS AUSTRALES

MOLECULAR GAS IN FOUR SOUTHERN BARRED SPIRAL GALAXIES

E. Bajaja

Instituto Argentino de Radioastronomía

RESUMEN: Se presentan los resultados obtenidos en la observación de cuatro galaxias espirales barreadas australes, NGC 613, NGC 1313, NGC 1566 y NGC 2442, con el SEST en la linea $^{12}CO(1-0)$. Las detecciones obtenidas han permitido confeccionar, para tres de las galaxias, mapas de la distribución de densidad superficial del gas molecular y del campo de velocidad. De este último se pudo derivar también la curva de rotación y la velocidad sistemática para cada una de ellas, así como las masas de gas y cinemática haciendo uso de los diagramas de posición-velocidad y de los perfiles globales. Sólo en el caso de NGC 1313 las detecciones fueron marginales impidiendo la confección de dichos mapas.

ABSTRACT: The results of the observations of four southern barred spiral galaxies, NGC 613, NGC 1313, NGC 1566 and NGC 2442, with the SEST, in the $^{12}CO(1-0)$ line, are presented. Mapping has been possible for three of the galaxies allowing the determination, for each of them, of the molecular surface density distribution and the velocity field, and, from this, the rotation curve and the systemic velocity. Other parameters like the gas mass and kinematical total mass, were also possible to determine from the position-velocity diagrams and the

global profiles. Only in the case of NGC 1313 the detections were marginal so no mapping was possible.

1. INTRODUCTION

The study of galaxies requires the knowledge of the parameters that define the physical conditions of each of their constituents. Basically, galaxies consist of three main components: stars, dust and gas, the last two being part of the interstellar medium (ISM). Stars are formed out of the ISM and this receives back part of it after being processed by the stars. There is, in consequence, a continuous physical and chemical interaction between both, stars and ISM, which makes of their compositions, distributions and kinematics, time dependent variables. The knowledge of these parameters then is the first necessary step for the study of the evolution of the galaxy as a whole.

The simplest way of learning about this evolution would be to study a sample of galaxies of the same type and different ages (i.e., at different distances). This is not directly possible, however, because of the difficulty in determining that two galaxies of different ages had identical initial conditions at the time of formation. The study of the evolution, anyway, requires modelling with the assumption of the initial conditions for every particular galaxy and, of course, a good knowledge of the processes of star formation and evolution for deriving the mass function of the formed stars and the physical and chemical interaction with the ISM along the whole existence of the stars.

The main components then, participating in this evolutionary process, are the hydrogen, the stars, and the products of the star burning returning to the ISM. The hydrogen is mostly present in three forms: as atomic, HI, molecular, H_2, and ionized, HII. The relative distribution of each of these three components on the galaxy is the result of the interactions mentioned above during the immediate past. The distribution of the three components put together, must represent the integration of the processes of star formation and interactions through the evolutionary history of the galaxy. These are two different aspects of the study of the galaxy. The first permits to understand the "present" state. The second the history. In any case, the knowledge of the distribution and kinematics of the three gaseous components is fundamental for both types of studies.

The HI can be traced very easily through the detection of its hyperfine transition at λ21 cm. Large efforts have been put observing this line on galaxies. In the northern hemisphere synthesis telescopes like the Westerbork Synthesis Radio Telescope (WSRT) and the Very Large Array (VLA) have been very productive and useful for mapping the HI with high angular resolutions (seconds of arc). From these maps a much better knowledge of the characteristics of this gas component has been gained, providing reliable information about the HI distributions, the velocity fields, the rotation curves, the streaming motions and their relationships with the other components (stars and dust).

In the southern hemisphere, there have been also many observations of HI in galaxies but, unfortunately, there has been not, till now, any synthesis telescope for this line. In consequence, for most of the spectacular southern galaxies, with the exception of the Magellanic Clouds, there are not yet high angular resolution HI maps, only global velocity profiles or, at most, for the largest ones, mappings based on a few grid points. Nevertheless, these observations provided useful information about the amount of gas, its mean velocity and the highest relative projected velocity (through the velocity width of the profile). Even a hint about the distribution of the HI on the galactic plane may be obtained from the shape of the velocity profile.

The HII is also easily detectable through the radio continuum originated in the free-free transitions of the electrons in that medium and optically through the Hα emission. With H_2 the situation is quite different. H_2 has no lines in the radio range. Radioastronomically it has to be detected indirectly through a related emitter. One of the components of the ISM that can be related to the H_2 is the CO molecule which has transitions between rotational levels in the millimeter range. Only in recent years, however, the technology reached the possibility of constructing radiotelescopes for millimeter waves with low noise receivers and dishes large enough to be able to detect the emission of the interstellar molecules that radiate at those wavelengths. The sizes of these telescopes are from 10 to 45 m and the rms deviations from the ideal parabolic surface are less than 100 μm.

The ^{12}CO molecule (we shall refer to it sometimes simply with CO) is abundant in the ISM and the detection of its $1 \rightarrow 0$ transition at λ 2.6 mm is relatively easy with the new radiotelescopes. With the mentioned telescope sizes the angular resolutions, at λ2.6 mm, are 230" to 10" . These resolutions are sufficient to resolve, on many nearby galaxies, features like the arms, the bars and, eventually, the nuclear regions. These resolutions are also comparable to those attainable with synthesis radiotelescopes at the HI λ21 cm line so the mass and velocity distribution for both forms of hydrogen can be directly compared, provided that the H_2 can be derived from the CO.

In the southern hemisphere, the Swedish-ESO Submillimeter Telescope (SEST), installed in the ESO Observatory at La Silla (Chile), is a 15 m telescope with a beam of 43" at the 2.6 mm wavelength of the $^{12}CO(1-0)$ transition. This beam is small enough to resolve the nearest galaxies (diameters larger than about 6´). With this telescope it is possible now to obtain high angular resolution CO maps of southern galaxies before any HI map of similar resolution is available. This will happen, however, in the near future when the

Australian Telescope starts to operate with a spectrometer. It will be possible then to compare both data.

The observation of southern galaxies with the SEST was started in 1988. A group of spiral galaxies were selected by several members of the Max-Planck-Institut fur Radioastronomie (MPIfR) in Bonn (FRA)[1] (including the author, at that time on leave at that Institute) for their observation in the $^{12}CO(1-0)$ line. The selection rules were the following. First, we wanted to map the galaxies in this line, so the probability of detection should be high. The best candidates are those where star formation is going on. This means that the galaxies should show dust, Hα emission, blue stars, IR, etc. Second, the angular sizes should be large enough to be able to resolve the main features (arms, bar, etc.) and, at the same time, small enough for keeping the observation time within reasonable limits. In addition, the inclination angles of the selected galaxies should be neither so low as to loose details of the velocity field nor so high as to loose details of the arms, and the declinations should be adequate for the SEST.

From the selected galaxies we have already observed NGC 613, NGC 1313, NGC 1566 and NGC 2442. These turned out to be all barred spirals of different types, which is consistent with the first condition since the bar, being a source of dynamical perturbations is also a source of shocks waves which may trigger the process of star formation. For all the observed galaxies, single dish HI line observations are available and three have been observed in the radio continuum, at 843 Mhz, with the Molonglo Observatory Synthesis Telescope (MOST) (Australia). These continuum observations were made with an angular resolution of 43" which happen to be the same as the resolution of the SEST at λ 2.6 mm, a very convenient coincidence.

[1] The following members of the MPIfR participated in this project: J. Harnett, E. Hummel, H.-P. Reuter and R. Wielebinski.

The fact that these galaxies are barred spirals adds interest to these observations. In spite of the fact that 43% of the galaxies catalogued by de Vaucouleurs et al. (1976) (BGCII) are of SB type and 31% SAB, the barred spirals are much less understood than the normal spirals. The reason for this is that the nearest ba- rred are farther than the nearest normals and the best exemplars of barred galaxies are visible only from the southern hemisphere. In consequence the results of these observations may turn out to be important for the study of this particular type of galaxies. Furthermore there is in general little HI emission from the bar itself and it is there where it is important to know the distribution and the velocity field of the gas in order to compare them with the models. These models predict the ocurrence of shocks due to the relative motions of the gas with respect to the bar boundaries. At least the dust lanes are consistent with those predictions. A problem, anyway, that has to be faced when dealing with bars is the fact that the presence of non-circular motions on them makes it difficult to determine the rotation curve and the local mass distribution.

We report here the basic results of the observations of the four mentioned barred spiral galaxies with the SEST in the λ2.6 mm of the $^{12}CO(1-0)$ line. This is a kind of summary of the observational and reduction work done and a display of the preliminary results. The data will be further processed and published individually for each galaxy. In the next two sections we describe the galaxies and the observations and in section IV the results.

2. THE GALAXIES

In Table 1 we list some of the main parameters of the four selected galaxies as were known before the observations with the

SEST. The coordinates are those of the nucleus as obtained from different optical and radio observations. The type, the diameter (D_{25}), the inclination (from R_{25}) and the systemic velocity (Vo) were taken from BGCII. The HI data are from Reif et al. (1982). As can be seen, the galaxies have angular diameters between 6 and 8 minutes of arc approximately and all of them are barred spirals of different types. We describe now, briefly each galaxy. Except otherwise stated, all quoted velocities in this paper are heliocentric and for the distance estimation a Hubble constant of 75 (km/s)/Mpc will be used.

Table 1

Optical and HI parameters of the observed galaxies

NGC	RA	Dec	Type	diam	i	PA	Vo	V_{HI}	V_{HI}	M_{HI}
	h m s	o ' "		'	o	o	km/s	km/s	km/s	Mo/Mpc
613	01 31 59.4	-29 40 27	SB(rs)bc	5.8	38	115	1500	1493	400	1.0
1313	03 17 39.0	-66 40 42	SB(s)d	8.3	40	170	448	475	199	10.2
1566	04 18 52.8	-55 03 24	SAB(s)bc	7.8	36	14-30	1394	1505	229	3.2
2442	07 36 33.0	-69 25 00	SB(s)b	6.9	24	40	657	1469	533	1.3

NGC 613

This galaxy, classified as SB(rs)bc in the BGCII, shows (Fig. 1a) that the nuclear region, the bar and the spiral arms are well defined. A ring-like feature is also present around the bar. The nuclear region contains bright HII regions which form spiral arms around a nucleus of 12" in diameter which seems to be composed of old stars. A prominent dust lane is seen along the bar and emission knots outline several arms to distances of about 100" from the center. The most active star formation appears to occur at the ends of the bar.

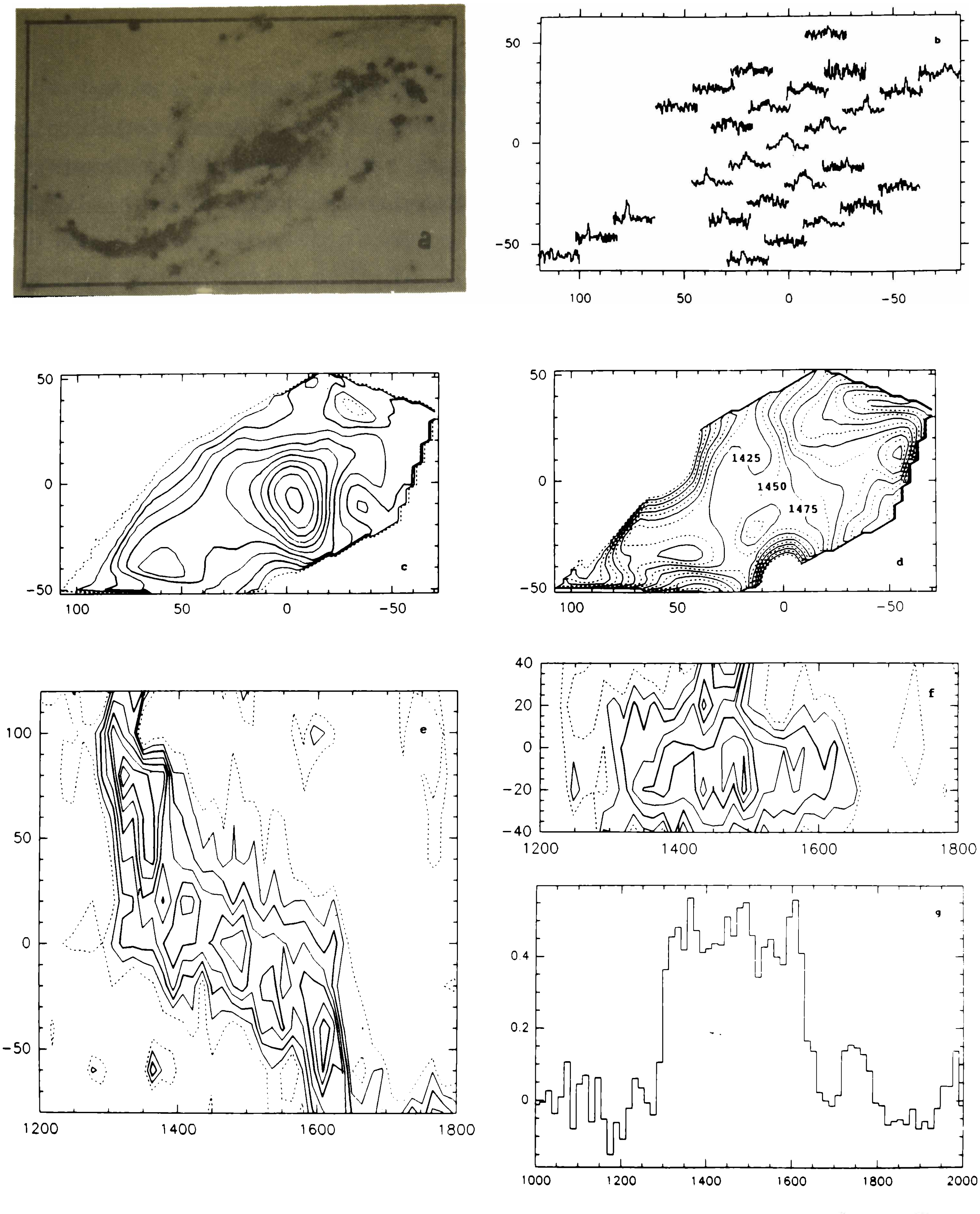

Figure 1: Display of the observational results for NGC 613: a) Optical picture, North at top, East at left. The rectangle reproduces the coordinates box of panel b. b) CO velocity profiles. The velocity range for each profile is 1000 to 2000 km/s and the velocity resolution is 14.4 km/s. The temperature scale is 0.025 K/mm. The coordinates are offsets with respect to the center in seconds of arc on sky. c) Contour map for the integrated intensities. First contour (dashed) level and contour interval are 1.5 K km/s. d) Velocity field. Contour interval is 25 km/s. e) Position-velocity diagram along the major axis (PA = 115°). First contour (dashed) level and contour interval are 0.01 K. Ordinates are offsets and in the abscissa the velocity is in km/s. f) As e) for the minor axis. g) Global velocity profile. Coordinates are temperature in K and velocity in km/s.

Optical spectra from this galaxy were obtained by Burbidge et al. (1964) who derived the rotation curve on the basis of prominent Hα, [NII] and [SII] lines. They used for the position angle the value of 115°. It has also been observed in the radio continuum at λ6 cm and λ20 cm with the VLA by Hummel et al. (1987) who detected jet-like features along the minor axis. They also made CCD photometry in the Hα and [OII]λ5007 lines finding the same kind of features which they interpreted as collimated ejections or outflows perpendicularly to the galactic plane.

HI global profiles were obtained by Bajaja (1978) and Reif et al. (1982) (hereafter B78 and RMGWS respectively) with the IAR and Parkes single dishes respectively. The sensitivity of the observations made with the Parkes radiotelescope were considerably higher than that of the IAR so in Table 1 the Parkes data were specified. IAR data are similar and the differences within the errors.

On the basis of a recession velocity of 1458 km/s, the distance is 19.4 Mpc so the linear scale on the galaxy is 94 pc/".

NGC1313

This galaxy (Fig. 2a), classified in the BGCII as SB(s)d, has been defined by Sersic (1968) as very complex. Its type is intermediate between the bright spirals of type SBc and the type represented by the Large Magellanic Cloud but the resemblance to this one is remarkable (Sersic, 1968). There are several blue knots scattered around the main body which account for a significative part of the light coming from the galaxy.

Marcelin and Athanassoula (1982) derived the velocity field from 8 interferograms in Hα. They obtained the velocity for 200 positions with a velocity resolution of 10 km/s. They found, from the velocity field, that the rotation center is outside the bar, 1.5 kpc south from the nucleus (a displacement of the rotation center had been previously indicated by Carranza and Aguero (1977), but in the opposite direction). They estimated the position angle of the major axis as 170° and the systemic velocity as 465 km/s. The PA of the bar is 11° ± 4° and the inclination of the galaxy 38°. Marcelin and Gondoin (1983) catalogued 375 HII regions which are found to be rather small, with an average diameter of 18.4 pc at 4.5 Mpc.

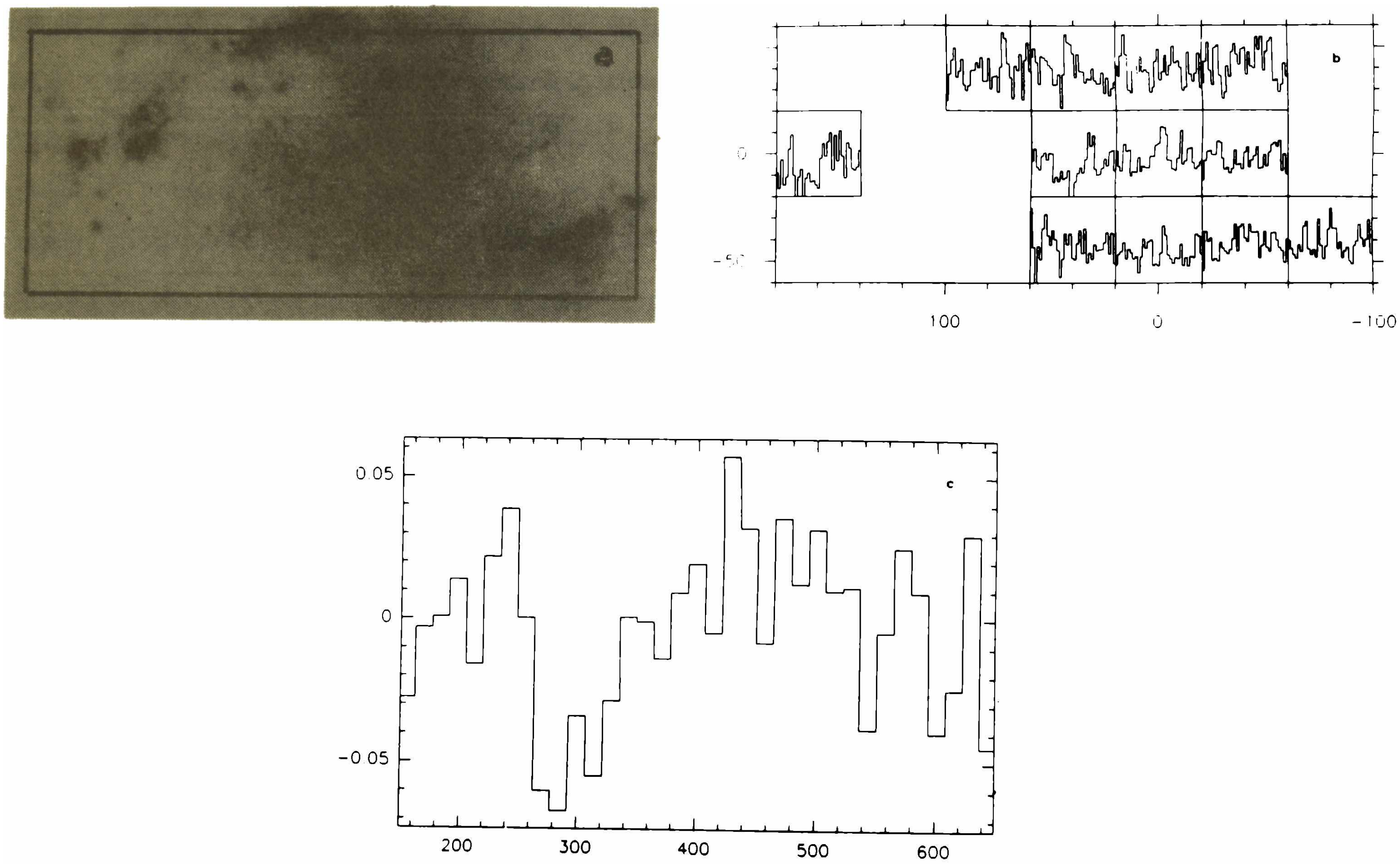

Figure 2: Display of results for NGC 1313. a) As in Fig. 1a. b) As in Fig. 1b. Velocity range 150 to 650 km/s and temperature scale 0.0042 K/mm. c) Global velocity profile.

Harnett(1987) observed this galaxy in the continuum at 843 MHz with the MOST. Extended radio emission is detected from the whole galaxy. There are also five radio peaks, one of them probably originated in a background source. This continuum map correlates very well with the FIR map at 100 μm obtained with the IRAS-CPC. There is very little dust visible in this galaxy.

B78 and RMGWS have observed NGC1313 in the λ 21 cm HI, both with good s/n ratio so their results are quite similar. The distance has been estimated by de Vaucouleurs (1973) as 4.5 Mpc. At this distance 1" represents 21.8 pc.

NGC 1566

Classified as SAB(s)bc in the BGCII, this galaxy (Fig.3a) is the brightest member in the Dorado group. Three regions can be distinguished: a) a central region in which the nucleus (whose characteristics, although weak and variable, suggest a Seyfert type) and the lens appear to be dominated by old population and a very weak bar structure may be recognized at PA 354° (de Vaucouleurs, 1973); b) an intermediate region with bright, broad arms, marked by knots of HII regions and stars, which start at the ends of the small bar, and c) a region in which narrow spiral arms are defined by blue knots. A fourth region might be defined by a pseudo ring which, according to de Vaucouleurs (1973), looks like the prolongation of the inner arms. This author derived different inclination and position angles for the inner and outer regions which suggests the presence of warps.

Comte and Duquennoy (1982) observed the Hα emission. They were able to catalogue, from narrow band plates, 418 HII regions which delineates the spiral arms. Three Hα interferograms permitted them to obtain 273 radial velocities and to map the velocity field. From these measurements they derived the systemic velocity (1500 ± 30 km/s) and a rotation curve. They concluded that the pseudo ring originates in the prolongation of the outer spiral pattern. They also derived different inclination and position angles for the inner and outer regions (45° and 14° within 8kpc and 40° and 30° outside, respectively).

Harnett (1984) observed NGC1566 with the MOST in the continuum at 843 MHz. The obtained map shows a rather smooth distribution of the radio emission peaked at the center and extending over the nucleus and the disk. HI global profiles with good s/n ratio were obtained by B78, RMGWS and Whiteoak and Gardner (1977). The HI parameters, as given by RMGWS, are shown in Table 1.

The recession velocity, about 1290 km/s, implies a distance of 17.2 Mpc and a linear scale on the galaxy of 83.4 pc/".

NGC 2442

This spectacular galaxy (Fig.4a), classified as SB(s)b in the BGCII, shows an asymmetric pattern. On the northern side, a narrow dust lane is seen projected against an also narrow, slightly curved, spiral arm which starts at the end of the bar.The southern arm is more curved and much less defined. The nucleus is relatively small and shows strong Hα emission (Carranza, 1967). The bar is surrounded by a clumpy distribution of dark and luminous matter.

NGC 2442 is member of a small group of galaxies in Volans. The systemic velocity quoted in the BGCII is 657 km/s. Sersic (1968) quoted 450 km/s and Bajaja (1978), from 21 cm HI line measurements, but low s/n ratio, 661 km/s. These are all low velocities consistent with the apparent proximity of the galaxy. The HI line measurements made by RMGWS with higher sensitivity, however, indicated a mean velocity of 1469km/s.

This much higher value was confirmed later by Bajaja and Martin (1985), also observing the HI line, who obtained a mean velocity of 1430 km/s. Our CO observations, in consequence, if successful, would be able to confirm the right systemic velocity.

NGC 2442 was observed in the continuum with the MOST, at 843 MHz, by Harnett (1984). The radio emission traces the main features of the galaxy, particularly the northern spiral arm. The radio continuum extends over the disk and the nucleus and shows three peaks, one at the center and one on each of the ends of the bar. There are no IRAS-CPC map for this galaxy. The position angle has been estimated, approximately, in 40°.

3. THE OBSERVATIONS

The observation of the $^{12}CO(1-0)$ line (λ2.6 mm), on the galaxies described in Section 2 were made with the SEST at the ESO Observatory in La Silla (Chile). The radiotelescope was dscribed by Booth et al. (1987, 1989a,b). At λ2.6 mm the 15 m telescope has a HPBW of 43", a beam efficiency of 0.78 and an aperture efficiency of 0.67. The dual polarization receiver, with cooled Schottky diode mixers, had a single side-band noise temperature of about 300 K. The Acousto-Optic Sepectrometer (AOS) consisted of 1728 channels spaced 690 kHz (1.8 km/s). The antenna temperatures Ta were determined using chopper-wheel calibrations. The pointing was checked, every hour, observing, generally, known SiO masers.

The observations of NGC 613 and NGC 1566 were made between the 25th and the 29th of July, 1988. NGC 1313 and NGC 2442 were observed between the 24th and the 29th of March, 1989. The observations were made in the beam-switch mode, integrating, on each cycle, 2 minutes on the source and 2 minutes on a position 12' off the source to the west. The total integration time for each observed point was, in general, 16 minutes (on the source), except in the case of NGC 1313, on which, due to the very low flux density of the CO signal, much more integration time (of the order of one hour per point) was spent.

Table 2

Observations

NGC	Grid Spacing "	Grid No. of points	P.A. °	Total int. time min
613	20	27	115	752
1313	40	13	0	912
1566	40	27	25	864
2442	20	69	40	1672

In Table 2 we have specified the grids and the total integration times for each of the galaxies. The spectra were reduced in the MPIfR and in the IAR using the software package developed in Grenoble (GAG). The baselines were removed in each case fitting polinomials of order 1 to 3, according to the extension of the signal-free base line. The spectra were smoothed to a velocity resolution of 14.4 km/s. The results displayed in Figures 1 to 4 are all based on this resolution.

4. RESULTS

In Figures 1 to 4 are displayed the main results of these observations for each of the four galaxies. We were able to map the CO emission detected on three of the galaxies. In the case of NGC 1313 the s/n ratio in the spectra, in spite of the amount of integration times, is so low that we may assume a marginal detection in only some of the observed points. Each figure, except Fig. 2, consists of seven panels: a) the optical picture, b)the velocity profiles on the observed grid points, c) the contour map, d) the velocity field, e) and f) the position-velocity diagrams along the major and minor axis respectively, and g) the global profile. In Fig. 2 only the velocity profiles (individual and global), besides the optical picture, are shown. All the figures, except those of panel a), were built with the GAG software. **Warning**: In the cases of panels c) and d) this software makes interpolations in regions where no observations have been made assuming that the signal is null only at the boundary of the whole region. In consequence those interpolations should be taken with care or simply ignored.

We shall analyze now the results for each galaxy. For the conversion of the velocity integrated CO temperatures, Wco, to the molecular column density, $N(H_2)$, we use the conversion factor X = 3 10^{20} cm^{-2} /(K km/s). This is a kind of mean value, with a possible error of 100%, of the several values derived by different authors, like Sanders et al. (1984) and Bloemen et al. (1986) and other quoted by them.

NGC 613

The distribution of the integration times is not uniform as is evidenced by the noise in the profiles of Fig 1b. The lowest noises occur in the spectra along the major axis. The concentration of the integration time on these grid points was due to their importance for deriving the rotation curve and the related parameters and also to the fact that they are located along the bar. From visual inspection it can be noticed that: a) The broadest profiles are at the center and at 20" to the SW along the minor axis; b) The profiles within ± 40" from the center along the major axis, are quite symmetric. In particular the two profiles at +40" and -40" are like a mirror image of each other and both show a narrow velocity component. c) The CO emission is asymmetrically distributed at distances larger than 40", with respect to the center, along the major axis. d) Along the minor axis the symmetry properties of the spectra can not be easily derived because of the much poorer s/n ratio. It is obvious, however, that there is more CO emission from the SW as from the NW. e) The profile at the extreme NE position, along the major axis, shows two velocity components. This position is in a region in which two arms appear to be crossing each other. The interpretation might be then that there are projection effects either due to warps or arms on different planes.

A better description of the CO distribution may be obtained from the integrated intensities which should be proportional to the H_2 column densities. This distribution is shown in Figure 1c and we remind here the warning, about the contour maps, made at the beginning of this Section. The figure shows that the maximum in the column density is displaced 13" to the SW, where nothing peculiar is seen on Fig. 1a. The contours indicate also an elongation along the minor axis resembling the ejection-like features detected by Hummel et al. (1987) in the radio continuum and in the Hα and [OIII] lines. If the molecular gas is distributed in the plane it would have an oval shape with an axial ratio of 2:1.

This picture is complemented by Fig. 1d which shows the velocity field of the mean velocity as obtained with the GAG software. Misleading effects caused by the interpolations outside the observed points are here more serious. Within the central region, however, where the velocity field should be more reliable, the contours show a rather wide plateau instead of the usual highest gradient which is displaced about 25" to the north. It is very improbable a displacement of the rotation center by this amount. A better insight in the velocity behaviour can be obtained analysing the position-velocity diagrams of Figs. 1e and 1f along the major and minor axis respectively. Between -20" and +20" along the major axis and between -40" and +10" along the minor axis the velocity profiles are about 400 km/s wide at 20% level. The velocity curve along the major axis can be well defined and it shows that in the central region, from -20" to +20", the velocity curve, as defined by the CO peak temperatures, can be described by a straight line with a steepness of about 3 (km/s)/".

The optical measurements by Burbidge et al. (1964) show that within about 10" from the center, there are circular velocities defined by a steep rotation curve with a total velocity range of also 400 km/s. The steepness in this case is about 18 (km/s)/". If there is CO associated to this central fast rotating feature, it is smeared out by the 43" beam of the SEST and that is reflected in the width of the central CO velocity profiles. These profiles have similar mean velocities and contribute to a plateau-like velocity field.

From the velocity curve of Fig. 1e, as defined by the temperature peaks, we can estimate the central velocity and the highest projected velocities with respect to the center. The central velocity is estimated as 1480 ± 5 km/s. At the SE, from +20" to +80" the velocity remains constant at 1358 km/s. Symmetrically, in the NW, between -20" and -80", the velocity is 1610 km/s. The average of these two velocities is 1484 km/s and the difference 252 km/s.

The position-velocity diagram along the minor axis (Fig. 1f) shows that at an offset of +40" (NE) the CO is seen, with much smaller velocity width, at the central velocity of 1480 km/s. We can assume, in consequence, that this velocity is the systemic velocity and the recession velocity 1442 km/s. The distance to the galaxy with the adopted Hubble constant, would be then Δ = 19.2 Mpc.

Between +40" and +120" there is another component in the velocity curve at about 1307 km/s. There might be a similar component, symmetrically placed at about 1660 km/s in the NW, with the same average and a difference of 354 km/s, but the observations did not go far enough. A projected velocity of 177 km/s with respect to the center (or a rotational velocity of 287 km/s, assuming an inclination angle of 38°), at a distance of 120", i.e., 11.2 kpc, permits a rough estimation (without any kind of correction) of the total mass within that distance. We obtain for this mass Mk = 2.1 10^{11} Mo.

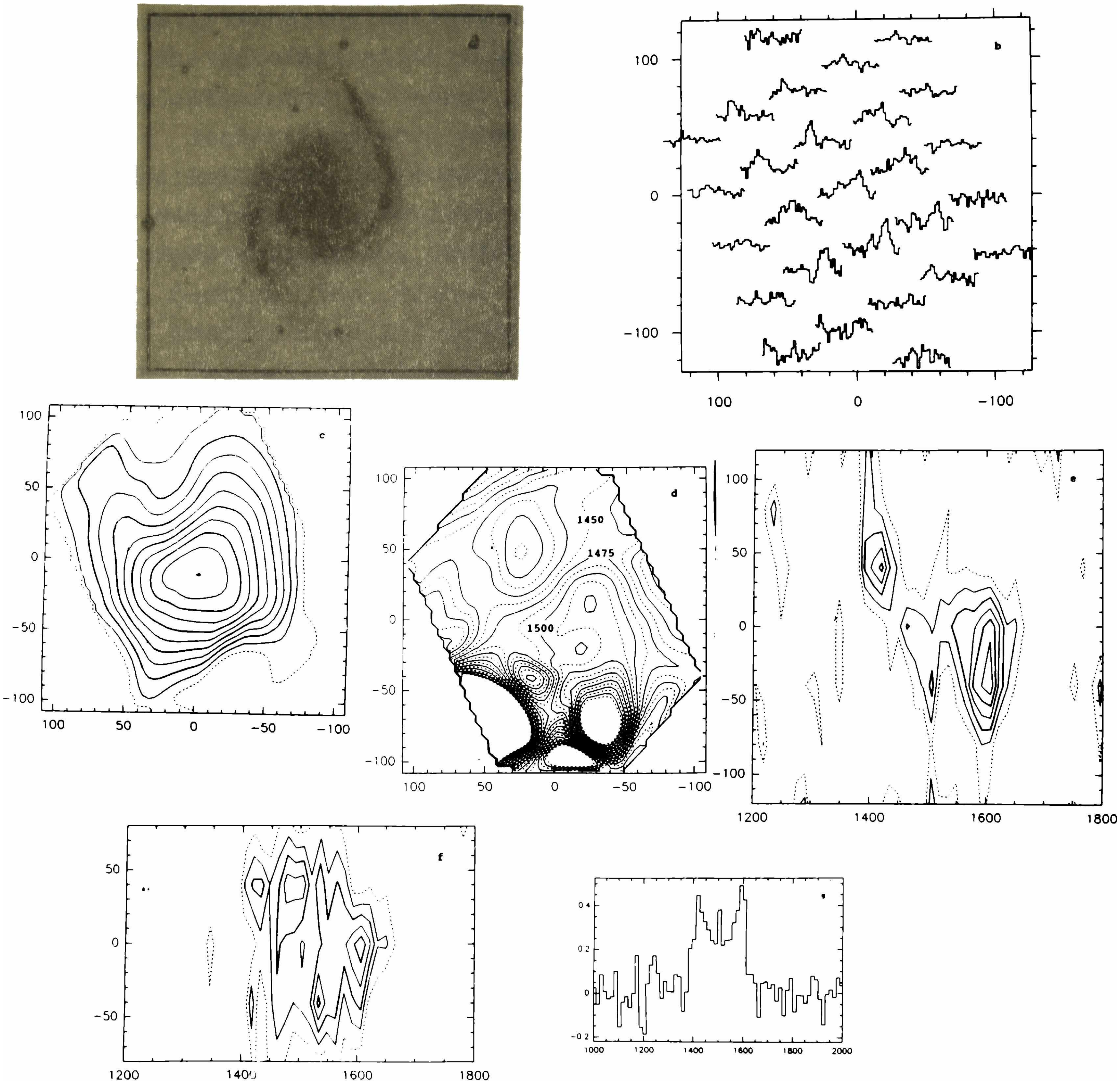

Figure 3: As Fig. 1. for NGC 1566. b) Velocity range 1300 to 1700 km/s and temperature scale 0.019 K/mm. c) First contour (dashed) level and contour interval are 1 K km/s. d) Contour interval is 25 km/s. e) and f) First contour (dashed) level and contour interval are 0.015 K. The major axis assumed to be at PA = 25

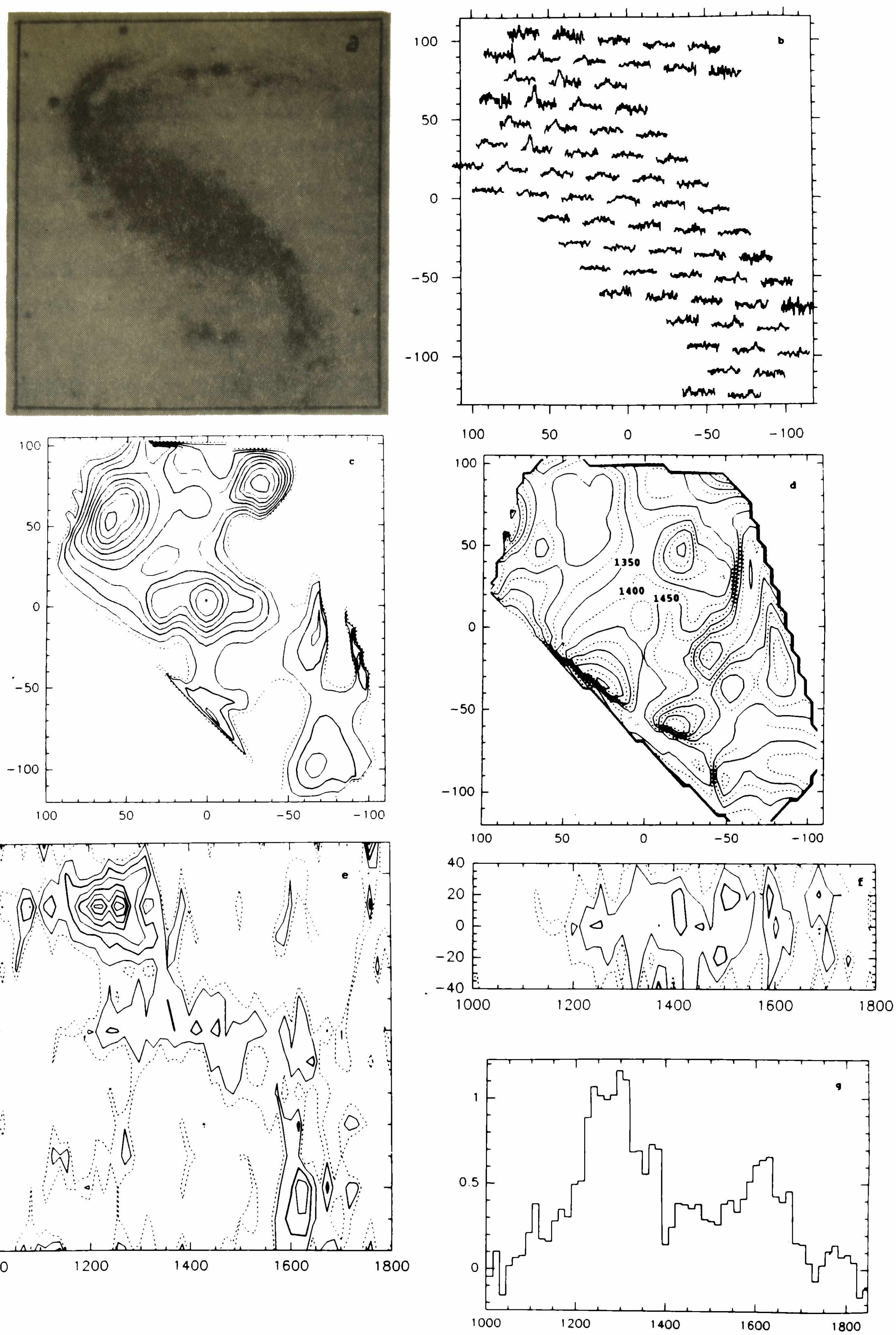

Figure 4: As Fig. 1, for NGC 1566. b) Velocity range 1000 to 1850 km/s and temperature scale 0.041 K/mm. c) First contour (dashed) level is 1.2 K km/s and contour interval is 1.5 K km/s. d) Contour interval is 50 km/s. e) and f) First contour (dashed) level is 0.01 K, second level is 0.02 K and the contour interval for the rest of the contours is 0.015 K. The major axis is assumed to be at PA = 40

Finally, from Figure 1g which shows the CO global profile, i.e. the result of adding up all the profiles of Figure 1b, we can obtain the integrated intensity Wco = 167 K km/s. The global profile, however, can be separated in two components, a main feature with W_1 = 153 K km/s, mean velocity V_1 = 1463 km/s and width $\Delta V1$ = 318 km/s, and a second one with W_2 = 24 K km/s, V_2 = 1750 km/s and ΔV_2 = 57 km/s. This second component is real and can be clearly seen in the central profile. From the total integrated intensity the H2 mass is $M(H_2)$ = 2.7 10 Mo. This H2 mass, as will be the case for the other galaxies too, is a lower limit since there is an underestimation due to the incomplete coverage of the surveys.

The HI global velocity profile obtained by RMGWS is very similar to the CO global profile of Fig. 1g in the shape and the width. The mean velocity is somewhat higher, 1493 km/s, but the difference is within the errors. The HI mass derived from this profile is $M(HI)=3.6\ 10^8$ Mo. In consequence, $M(H_2)/M(HI)$= 0.75 but, in view of the uncertainties and the underestimation in the derivation of $N(H_2)$, we can simply say that both masses are similar.

NGC 1313

Figure 2b shows the velocity profiles obtained from the observation of this galaxy. In Table 3 we have listed the integration times spent on each grid point as well as the parameters derived from each profile. The spacing between the points is 40" so the spectra are practically uncorrelated. The positions of the observed grid points were selected in order to have them on the center, on some blue knots and on regions of enhanced FIR as depicted by the IRAS-CPC maps.

We are inclined to believe that the features seen in the spectra at offsets (in seconds of arc) (-80,-40), (0,0), (40,0), (40,40) and (80,40), correspond to CO emission. All these features have poor s/n ratio but their velocities, between 380 and 490 km/s, are compatible with the range of velocities measured in Hα by Marcelin and Athanassoula (1982) and in HI by B78 and by RMGWS (360 to 575 km/s).

The low s/n ratio for each individual profile and the differences in the velocities make it difficult to recognize any feature in the global profile of Figure 2c. If we assume that the global profile is similar to the HI profile, as obtained by B78 and RMGWS, at least in the width, then the apparent feature buried in the noise, between 360 and 580 km/s, might be real. The parameters of this feature are: mean velocity 464 km/s, velocity width 245 and integrated intensity, W_{CO}, 0.48 K km/s. Using for the distance the value of 4.5 Mpc given by de Vaucouleurs (1973), the H_2 mass would be then $M(H_2) = 1.7\ 10^6 M_\odot$.

The HI mass as given by RMGWS is $M(HI) = 1.3\ 10^9\ M_\odot$ so the ratio $M(H_2)/M(HI) = 1.3\ 10^{-3}$. For this late type galaxy, however, it could happen that the conversion factor X is much higher than for normal spirals. Dettmar and Heithausen (1989) found, for NGC 55, a value 20 times higher than the one used here. Also for the Large Magellanic Cloud it is 6 times higher (Cohen et al., 1988). Using for X a value 20 times higher, $M(H_2) = 3.4\ 10^7\ M_\odot$, still a very low value.

It must be noticed that the velocities of the apparent individual CO features do not agree strictly with the velocities measured in Hα by Marcelin and Athanassoula (1982) at the same positions. Also the CO profiles do not show symmetry with respect to the center. So the doubt persists whether we have detected any CO at all.

Table 3

NGC 1313 spectra parameters

Offsets "	Offsets "	τ min	σ 10^{-4} K	Tp K	Vp km/s
-80	-40	80	61	0.019	399
-40	-40	80	54	0.010	420
0	-40	96	50	0.009	427
40	-40	40	79	-----	---
-40	0	80	55	-----	---
0	0	96	54	0.016	411
40	0	80	69	0.013	485
-40	40	48	96	-----	---
0	40	112	75	-----	---
40	40	76	58	0.020	355
80	40	48	77	0.021	488
160	0	132	94	-----	---
-200	-120	16	126	-----	---

NGC 1566

The whole extension of the bright arms of this galaxy has been observed using a grid spacing of 40". The integration times are, in general, 16 minutes on the source so the noise on all the spectra are more or less the same (about 0.01 K) as can be seen in Figure 3b. The visual inspection of the CO profiles permits to appreciate a high degree of symmetry with respect to the center, as well in the velocity structure as in the amplitudes. A good correlation can also be seen between the arms and the CO signal. This correlation is seen better in the contour map of Figure 3c which represents the distribution of the molecular component in the galaxy.

The distribution is peaked in the center but the peak itself is shifted 10" to the south. Since the grid spacing used for this galaxy means an undersampling for a 43" beam, and the position of the peak has been determined by the interpolation procedure of the GAG software, the amount of the shift might contain an appreciable error. The fact, however, that the other contours keep the symmetry around this peak seems to indicate that the shift is close to the real one. The contours shows, furthermore, an oval shape with its major axis oriented along the minor axis of the galaxy. Both effects, the shift of the peak and the oval distorsion, have appeared also in the case of NGC613. The outer distorsions of the contours to the north and the south indicate a correlation with the thick arms but similar distorsions towards the NE and the SW are not correlated with any optical feature.

The velocity field displayed in Figure 3d shows a kind of standard velocity field in the northern part of the galaxy but the isovelocity lines seem to indicate a rotation center 30" to the north of the galactic center. The position-velocity diagram along the major axis of Figure 3e does not help to derive the velocity curve. This diagram shows a narrow component, at about the systemic velocity along the observed southern part of the major axis and up to 80" along the northern part. This component is not seen along the minor axis but here the situation is still worse because, from -50" to +50" up to 4 velocity components are visible there. We recall here that de Vaucouleurs (1973) and Comte and Duquennoy (1982) derived different position and inclination angles for the inner and outer regions of the galaxy. We adopted here an intermediate value of 25° for the position angle.

If the velocity curve is determined by the strongest CO peaks in Fig. 3e, then the central velocity is 1513 km/s. The projected velocities at 40" from the center are 1419 and 1605 km/s with a difference of 186 km/s and an average of 1512 km/s, almost identical to the central velocity. Adopting 1512 km/s for the systemic velocity, the recession velocity would be 1296 km/s and the distance 17.3 Mpc. At +120" the projected velocity is 1396 km/s so, assuming an inclination angle of 36° , the circular velocity, at that distance from the center, is 197 km/s. From the distance and the circular velocity we can estimate, like in the case of NGC 613, the total mass, within 9.9 kpc, as 9.1 10^{10} $M_{\odot}$.

Figure 3g shows the CO global profile. It is quite symmetric and 2-horns shaped, with steep sides. It shows clearly the narrow component at the central velocity seen in Fig. 3e. It is very similar to the HI profiles as obtained by B78 and RMGWS. The mean velocity is 1512 km/s, the width 222 km/s and the integrated intensity 75.4 K km/s. From this integrated intensity we can estimate the H_2 mass $M(H_2) = 4.1\ 10^8\ M_\odot$ and the ratio $M(H_2)/M(HI) = 0.43$. **NGC 2442**

We started the observation of this galaxy centering the spectrometer at the low velocity quoted in the BGCII (see Section 2). In view of the lack of detection we tried then the higher velocity, given by RMGWS and Bajaja and Martin (1985), with immediate success, so we kept this velocity for the whole survey. As in the case of NGC 1566, this galaxy was observed with a rather uniform distribution of integration times, in general 16 min. on the source for each point. The grid spacing in this case, however, was 20", i.e. a correct sampling for the 43" beam of the SEST. Most of the visible part of the galaxy was observed, obtaining 69 spectra which are shown in Figure 4b. From visual inspection of the profiles it is possible to conclude: a) The CO signal is not symmetrically distributed with respect to the center. The peak temperatures are more than two times higher in the NE than in the SE. b) In the center the peak temperatures are lower than in the NE and SW but the profiles are much broader.

The contour map produced with the integrated intensities of the profiles of Fig. 4b are shown in Figure 4c (see warning at the beginning of this Section). This map shows three peaks in the CO distribution along the major axis, the strongest in the NE, the weakest in the SW and an intermediate one at the center. The latter shows an oval shape with its elongation oriented in the E-W direction. A fourth peak appears in the NW, over the narrow arm and well defined dust lane, where the profiles are also quite broad. The contours in this region do not show the real distribution because of the limited number of points.

The corresponding velocity field displayed in Figure 4d, even simplifying it, bearing in mind the above mentioned warning, shows a complicated pattern due mainly to regions with very low s/n ratio which makes the velocity values quite uncertain. In the regions where the s/n ratio is higher, the isovelocity lines are smoother and better defined. These velocities, however, do not show the real complexity of the velocity structure. This can be better appreciated in the position-velocity diagrams of Figures 4e and 4f.

From the diagram for the major axis (Fig. 4e) it can be concluded: a) There is a very steep velocity gradient at the center as shown by the profiles at offsets -20", 0" and +20". The gradient is about 22 km/s/". b) The velocity of the center may be estimated as 1435 ± 10 km/s. c) The velocity at the southern end of the major axis may be estimated as 1618 km/s. d) The velocity in the northern end should be, under symmetrical conditions, 1252 km/s, but this is just one of four components appearing on a broad profile at 80" from the center. At 100" there appears to be a cut off in the CO signal.

Along the minor axis (Fig. 4f) a broad velocity feature is also present. It corresponds to a central velocity field picked up by the beam also at -20" and +20". A velocity gradient is also seen in this case with a similar magnitude, 24 km/s/", which can not be understood if the broad velocity profile is due to a fast rotation around the center and on the plane of the galaxy. From this figure a shift of 7.5" of the rotation center might be possible but along the minor axis towards the SE.

The CO global velocity profile of Figure 4g shows that its total width is of the order of 600 km/s, occupying most of the available velocity range of the spectrometer. This may suggest baseline removal difficulties. The profile is not single peaked, there are two main components with different amplitudes and the sides are not steep. This shape for the global velocity profile is a consequence of asymmetry in the CO distribution seen in Fig. 4b. The HI profiles obtained by RMGWS and Bajaja and Martin (1985) are also broad but not as much as in CO. They do not show the two components structure but the s/n ratio is low in both cases and, certainly, there must have been problems with the baseline removal.

Because of all these problems, the mean velocity of each of these global profiles do not give the systemic velocity and the central velocity may have a large error because of the baseline uncertainty. The area of the global profile is also subject to these errors but in a less sensible way. The velocity integrated intensity is 313.4 K km/s. Adopting for the systemic velocity 1435 km/s, the recession velocity is 1161 km/s and the distance is 15.5 Mpc, so the H_2 mass is $M(H_2)$ = 3.2 10^9 $M_\odot$ and the ratio $M(H_2)/M(HI)$ = 1.0.

The projected velocity of 1618 km/s, at 120" from the center along the major axis, represents a circular velocity of 450 km/s assuming an inclination angle of 24° . The total mass within 9 kpc can be estimated, as in the previous cases, as M_K = 4.2 10^{11} $M_\odot$.

CONCLUSIONS

We have observed four southern barred spiral galaxies, NGC 613, NGC 1313, NGC 1566 and NGC 2442, in the $^{12}CO(1-0)$ line (115 GHz, λ2.6 mm) with the SEST. With the obtained detections we have been able to map the CO emision of three of the galaxies and we got marginal detections in the case of NGC 1313.

For each of the mapped galaxies we produced a contour map for the CO integrated intensity and for the velocity field, position-velocity diagrams along the major and the minor axis, and the global velocity profile. These displays permitted us to derive, for each galaxy:

a) The distribution of the molecular gas surface density.

b) The mean-velocity field of the molecular gas.

c) The velocity curve along the major axis and, from this, the rotation curve for the galaxy.

d) The central (systemic?) velocity, V_{sys}.

e) The velocity integrated intensity, or profile area, W_{CO} (K km/s).

f) The total width of the global velocity profile and the highest projected velocity.

The parameters derived from these observations are: the distance to the galaxy, Δ (Mpc), the mass of the molecular gas, $M(H_2)$ ($M_\odot$) and an estimation of the total mass from the rotational velocity at certain distance from the center, M_K ($M_\odot$).

These parameters, together with the blue luminosity, L_B, as quoted by RMGWS, are listed in Table 4 in which the ratios $M(H_2)/M(HI)$ and $M(H_2)/L_B$ are also included for the 4 galaxies. We have confirmed the high value for the systemic velocity of NGC 2442 as found with observations in the HI 21 cm line. This implies a distance of the order of 15 Mpc. The velocity width shown by this galaxy is the largest observed in this sample, about 550 km/s, which, corrected for the low inclination, gives a width of 1350 km/s.

We have obtained quite different values for the velocity integrated intensity, W_{CO}. The highest value again correspond to NGC 2442 and the lowest to NGC 1313. In the latter, a large value for the factor which converts the W_{CO} to the H_2 column density, $N(H_2)$, could be responsible for the low value of W_{CO}. It is obvious anyway that the CO is closely related to the presence of dust and star formation.

The presence of the bar might be responsible for the very wide velocity profiles in the centers of the galaxies as evidenced in the position-velocity diagrams of the three mapped galaxies. Each of these show also an oval distribution of the CO emission with the peak displaced from the center of the galaxy and the elongation aligned rather with the minor axis of the galaxy. In the case of NGC 613, the latter feature is shared by the radio continuum and the [OIII].

The ratios $M(H_2)/M(HI)$ and $M(H_2)/L_B$ are distance independent so at least one very important uncertain factor does not play a role in the derived quantities. Still, due to the uncertainty in the CO to H_2 conversion factor, variations of even an order of magnitud can be meaningless. The values for these ratios in Table 4 show that those for NGC1313 are very different from the rest, and in this case the difference is meaningful.

Table 4

Parameters derived from the CO observations

NGC	Vsys km/s	ΔV km/s	Ico K km/s	Δ Mpc	M(H2) 10^8Mo	Mk 10^{10}Mo	M(H2)/ M(HI)	LB 10^9Lo	M(H2)/ LB
613	1480	360	167.1	19.2	27	21	0.75	36.2	0.075
1313	464	245	0.48	4.5	[0.0017]	--	[0.0013]	8.1	[2.1 10^{-4}]
1566	1512	275	75.4	17.3	41	9.1	0.43	15.6	0.263
2442	1435	550	313.4	15.5	32	42	1.0	23.4	0.136

Acknowledgments

The participation in this project, the observations with the

SEST and part of the reductions, made at Bonn, have been possible thanks to a grant from the Max-Planck Institut and to the European Southern Observatory. The observations were carried out with the cooperation of J. Harnett (NGC 1566) and H.-P. Reuter (NGC 1313 and NGC 2442).

REFERENCES

Bajaja, E. (B78): 1978, Publ. del Depart. de Astron. de la Univ. de Chile **111**, 55.

Bajaja, E., Hummel, E.: 1989, Messenger **55**, 37.

Bajaja, E., Martin, C.M.: 1985, Astron. J. **90**, 1783.

Bloemen, J.B.G.M., Strong, A.W., Blitz, L., Cohen, R.S., Dame,T.M., Grabelsky, D.A., Hermsen, W., Lebrun, F., Mayer-Hasselwander, H.A., Thadeus, P.: 1986, Astron. Astrophys. **154**, 25.

Booth, R.S., De Jonge, M.J., Shaver, P.A.: 1987, Messenger **48**, 2.

Booth, R.S., Delgado, G., Johansson, L.E.B., Murphy, D.C., Olberg, M., Whyborn, N.D., Greve, A., Hanson, B., Lindstrom, C.O., Rydberg, A.: 1989a, Astron. Astrophys. **216**, 315.

Booth, R.S., Johansson, L.E.B., Shaver, P.A.: 1989b, Messenger **57**, 1

Burbidge, E.M., Burbidge, G.R., Rubin, V.C., Prendergast, K.H.: 1964, Astrophys. J. **140**, 85.

Carranza, G.J.: 1967, Observatory **87**, 38.

Carranza, G.J. Aguero, E.L.: 1974, Observatory **94**,7.

Carranza, G.J., Aguero, E.L.: 1977, Astrophys. Sp. Sci. **46**, 23.

Cohen, R.S., Dame, T.M., Garray, G., Montani, J., Rubio, M., Thadeus, P.: 1988, Astrophys. J. (Letters) **331**, L95.

Comte, G., Duquennoy, A.: 1982, Astron. Astrophys. **114**, 7.

Dettmar, R.-J., Heithausen, A.: 1989, Astrophys. J. **344**, L61.

Harnett, J.I.: 1984, Month. Not. Royal Astron. Soc. **210**, 13.

Harnett, J.I.: 1987, Month. Not. Royal Astron. Soc. **227**, 887.

Hummel, E., Jorsater, S., Lindblad, P.O., Sandquist, A.: 1987, Astron.Astrophys. **172**, 51.

Marcelin, M., Athanassoula, E.: 1982, Astron. Astrophys. **105**, 76.

Marcelin, M., Gondoin, Ph.: 1983, Astron. Astrophys. Supp. Ser. **51**, 353.

Reif, K., Mebold, U., Goss, W.M., van Woerden, H., Siegman, B. (RMGWS): 1982, Astron. Astrophys. Supp. Ser. **50**, **451**.

Sanders, D.B., Solomon, P.M., Scoville, N.Z.: 1984, Astrophys. J. **276**, 182

Sersic, J.L.: 1968, "Atlas de Galaxias Australes", Córdoba.

Vaucouleurs, G. de: 1963, Astrophys. J. **137**, 720.

Vaucouleurs, G. de: 1973, Astrophys. J. **181**, 31.

Vaucouleurs, G. de, Vaucouleurs, A. de, Corwin, H.C.: 1976, "Second Reference Catalogue of Bright Galaxies" (BGCII), The University of Texas Press, Austin.

Whiteoak, J.B., Gardner, F.F.: 1977, Austr. J. of Physics **30**, 187.